Desalination and Water Treatment
www.deswater.com

doi: 10.5004/dwt.2021.26656

214 (2021) 146–154
February

Polymer membranes from polyvinylidene fluoride or cellulose acetate improved graphene oxide used in the UF process

Elwira Tomczak*, Martyna Blus

Faculty of Process and Environmental Engineering, Lodz University of Technology, Wolczanska 213/215, 90-924 Lodz, Poland, Tel. +48-42-6313708; email: elwira.tomczak@p.lodz.pl

Received 26 March 2020; Accepted 21 August 2020

ABSTRACT

In this paper, the study aimed at comparing laboratory-produced membranes from two different polymers containing graphene oxide (GO). The membranes according to the phase inversion method using commercial graphene oxide (2 mg/100 g matrix) were produced. Due to GO properties, it is possible to improve the permeability of the membrane concerning the macromolecular compounds, and increasing the permeate flux. The polymer matrix was formed from polyvinylidene fluoride (PVDF) or cellulose acetate (CA) dissolved in dimethylacetamide or acetic acid (AA), respectively. Polyethylene glycol (PEG), was used as a plasticizer. The membranes were evaluated by determining their thickness, Young's modulus, tensile strength at break, and pore size distribution. The presence of the GO in the membrane causes an increase in hydrophilicity of the surface, which was expressed by decreasing the contact angle from 77° to 43° for the PVDF/GO, and from 60° to 36° for the CA/GO membranes. The permeability, membrane resistance, and retention of the produced membranes for water and bovine serum albumin (BSA) in the ultrafiltration process using an OSMONICS KOCH apparatus under transmembrane pressure ranging from 0.1 to 0.6 MPa at 25°C was determined. It was obtained that membranes with GO have an appropriate pore size distribution for the UF process. The highest permeability (J_v = 0.13 $m^3/(m^2\ h)$), good rejection reaching over 90% for BSA initial concentration C = 0.75 g/dm^3 was reached.

Keywords: Polyvinylidene fluoride; Cellulose acetate; Graphene oxide; Bovine serum albumin; Ultrafiltration

1. Introduction

The membrane technology searches for materials allowing ultrafast and efficient permeation. Researchers look to test new polymers, and mainly modify the existing materials through physical and even more often chemical treatment.

It has been found that this is possible by adding nanoparticles to the polymer matrix.

In the last decade, considerable attention has been paid to membranes functionalized with various nanoparticles [1–3] and carbon derived nanomaterials such as carbon nanotubes, graphene, and graphene oxide [4–7]. After numerous studies, scientists focused mainly on the use of GO as an additive to membranes [8,9]. Graphene oxide has an amorphic structure, but its properties are dependent on the type and distribution of functional groups containing oxygen such as the hydroxyl, carboxyl, and epoxy group [10,11].

The structure and tunable physicochemical properties of graphene oxide offer an exciting opportunity to create a fundamentally new class of sieving polymer membranes.

Polyvinylidene fluoride (PVDF) is one of the popular membrane materials due to its outstanding properties including thermal stability, chemical resistance, and excellent

* Corresponding author.

mechanical strength [12–14]. The PVDF membranes are most commonly used for water purification in the ultrafiltration process to remove contaminations such as polysaccharides, proteins, dyes, organic compounds, and humic acids [15–19]. An extensive overview of the use of PVDF for the production of membranes was presented in a previous paper [20]. As the subject of the research is still important, further reports on the production of membranes, mainly PVDF/GO, are presented below.

Zhang et al. [15] in their research the contribution GO functional groups to reversible or irreversible fouling of two polysaccharides on the PVDF/GO membrane were investigated. They stated that modification of PVDF membrane using GO creates a more hydrophilic surface, and indeed decreases the fouling of polysaccharides. At the same time, they state that the contribution of functional groups to membrane fouling is still to be found, and the exact fouling mechanism is yet not confirmed and clarified.

Among novel methods, adding nanomaterials into PVDF/GO or PVDF polymer matrix is gaining in importance. An example of this is the incorporating TiO_2 nanoparticles into the membrane to increase the membrane's hydrophilicity, which consequently leads to an increase in water permeability [21]. Evaluating TiO_2-GO/PVDF hybrid membranes, the authors concluded that the water flux and antifouling performance first increased and then decreased with the increasing TiO_2 content in both TiO_2-GO and PVDF membranes. Therefore, the membrane composition should be always optimized.

In the work [22], PVDF ultrafiltration membranes with the direct blending of polyethylene glycol (PEG), methyl ether methacrylate grafted SiO_2 nano-particles in the casting solution by phase inversion method were synthesized. The modified membrane with 0.5 wt.% of SiO_2-g-PEGM nanoparticles showed enhanced porosity, pore density, pore area, pure water flux, and permeability. It was observed in the UF study that reversible and total fouling were decreased and achieved a high flux recovery ratio for this membrane. Studies showed a significant rejection of humic acid, bovine serum albumin (BSA), and oil–water emulsion on modified membranes compared to a normal membrane. The percentages rejection of HA, BSA, and o/w emulsion were increased from 90% to 94%, 71% to 91%, and 69% to 89%, respectively.

In the paper [14], a hydrophilic nanomaterial graphene oxide grafting poly *N*-isopropyl acrylamide was synthesized by atom transfer radical polymerization method and incorporated with PVDF. The dispersed GO (0.2%) in nanocomposite membranes with better thermo-responsing flux, higher water recovery ratio, BSA rejection ratio, and antifouling performance were compared with the plain membrane. It can be found that the BSA rejection ratio of blended membranes obtained a decline, but the effect at 25°C was better than at 40°C. The flux recovery ratio of all tested membranes was more than 51.5%.

The polyethersulfone/sulfonated polysulfone/graphene oxide (PES/SPSf/GO) with enhanced permeability, antifouling, and antibacterial properties were prepared by the non-solvent induced phase separation and characterized in the work [9]. The authors inform that they obtained pure water flux of fabricated membranes with a very low GO content of 0.012 wt.% was up to 816.9 L/(m^2 h) and the rejection of BSA was more than 99.2% under a pressure of 0.1 MPa. Additionally, the membranes high antifouling recovery (94.2%) and antibacterial performance (antibacterial rate (90.0% against *Escherichia coli*) were demonstrated.

Similar issues concerning the preparation of antibacterial and hydrophilic membranes scientists discussed in the article [23]. These studies report a novel method of synthesis of quaternized GO and applied it's as a modifier of the PVDF membrane surface. Antibacterial property fabricated membrane against *E. coli* has been shown. The number of bacteria was significantly reduced by over 99% which confirms strong antibacterial property.

The hydrophilicity of the membrane surface is assessed by water contact angle measurements.

It was obtained that with the increase of GO content to 0.1 wt.%, the contact angle decreased from 77.1° to 55.4°, but the GO concentration increased to 0.15 wt.% the contact angle increased to 60.6° again. Increasing the amount of GO in the membrane (0.05, 0.1, and 0.15 wt.%) caused a change in water fluxes to 1,078; 1,285; and 981 L/(m^2 h). In the presented experiments, BSA was used as a contaminant to evaluate the fouling resistance. So, it was proved that the flux recovery rate (0.1% GO) was 85.6%, which is significantly higher than that of the non-modified membrane (74.14%).

Although membranes made of PVDF with the addition of nanoparticles are usually used in pressure separation processes such as microfiltration, ultrafiltration, or even reverse osmosis, the possibility of their use in other membrane techniques is checked [24]. An example of this could be the work [25] regarding PVDF/GO membranes in membrane distillation. In this work reduced GO nanoplatelets with different degrees of reduction (36%, 58%, and 69% removal oxygen) were incorporated in the PVDF matrix. The highest porosity value of 70.1% was obtained for the membrane with 0.5 wt.% GO loading. Membrane distillation studies were carried out using NaCl solution of 35 g/L. The feed temperature was 80°C, the condenser plate was maintained at 20°C. The water flux and salt rejection values obtained throughout 2 h. The rejection of NaCl was almost 100% for all 10 prepared membranes. Another major finding in the presented work is the good performance stability of these membranes under a longer testing time of 96 h.

Cellulose acetate (CA) is a frequently used polymer for membrane production due to its easy preparation and low price while maintaining the proper properties of membrane sheets [26–28]. In the work [29], the effect of graphene oxide nanoparticles and polyoligosilsesquioxanes (POSS) on reverse osmosis efficiency was investigated using mixed matrix membranes. Cellulose acetate nanocomposite membranes with different GO and POSS content were prepared by phase inversion. Due to the unique properties of GO and POSS, the presence of nanoparticles and the working pressure turned out to be the main parameters affecting membrane performance in relation to salt rejection and water permeation flux. The GO and POSS nanoparticles accumulated in the polymer matrix, creating wider pores, which increased the water flow through the membrane.

The best results were obtained for a membrane containing 0.005 wt.% GO and 0.75 wt.%. POSS at an operating

pressure of 1.92 MPa. The permeation flux of 13.65 L/(m^2 h) and salt rejection of 77.83% were received.

In the study [30], the effect of adding different amounts of graphene oxide to the cellulose acetate matrix on desalination using reverse osmosis process was tested. GO content, feed salinity, and applied pressure were identified as main parameters in controlling the membrane efficiency. The presence of GO in the RO membrane increased its hydrophilicity, which resulted in increased water flux. The best results for water desalination were obtained for a membrane containing 0.009 wt.% of GO, with feed salinity of 3,500 ppm and using a pressure of 18 bar. A satisfactory the permeation water flux of 11.42 L/(m^2 h) and salt rejection of 58.08% were obtained.

In the work [31], the cellulose acetate/PEG membrane was prepared using a surface coating method. The polymer matrix was enriched with the graphene oxide in the range from 0.0025 to 0.0125 wt.% to the mass of the solvent. The membrane permeability and salt retention were analyzed. It was proved that the best results were obtained for a membrane containing 0.01 wt.% graphene oxide – a permeate flux of 1,356 L/(m^2 h), membrane permeability of 0.0013 L/(m^2 h kPa), and salt rejection of 37% were obtained. Analysis of the scanning electron microscopy (SEM) images determined that the membrane was asymmetrical, with a spongy structure. Analysis of the Fourier transform infrared (FTIR) results proved that the peak area of –OH bonds decrease with the addition of GO, which was also confirmed by reducing the contact angle.

In the study [32], the cellulose acetate UF membranes were prepared by the phase inversion method. To improve membrane properties, they were enriched with graphene oxide and HKUST-1(metal-organic framework)@GO. The effect of both additives on membrane morphology, permeability, separation ability, and anti-fouling properties were compared. It has been proved that CA/MOF@GO membranes show higher surface hydrophilicity, higher water flux, and smoother surface and larger pore channels also. This is due to the fact that HKUST-1 can take full advantage of the GO structure and prevent it layering. The highest water flux of 188.51 L/(m^2 h) was observed for the CA/MOF@GO membrane with the 0.12 g addition of carbon nanostructure. The good BSA rejection (91.36%) and better antifouling properties was also achieved for this membrane.

After careful analysis of the subject literature, the main objectives of the work were formulated. First, this study aimed to present the methodology of membrane production method, and second was to establish the proper composition of membranes produced from two different polymers with the addition of graphene oxide. The goal was to obtain membranes showing high permeability and a high retention coefficient for the selected protein solution. The choice of polymer should provide greater stability and mechanical strength, and the addition of GO increase membrane permeability. The membranes produced with and without the addition of graphene oxide were characterized by calculating their permeation flux, mass transfer resistance for water, and BSA solution. Finally, the rejection for BSA in the ultrafiltration process was also determined.

2. Preparation of the membrane

2.1. Materials

The membranes were produced via the phase inversion method with or without GO addition.

The active layer of the polymer matrix was made of PVDF or cellulose acetate (CA) dissolved in dimethylacetamide (DMAC) or acetic acid, respectively. PEG was employed as a plasticizer in both cases. GO nanoparticles in form of nanoflakes were distributed in the whole volume of the polymers. All reagents were purchased from Sigma-Aldrich (USA).

2.2. Laboratory formation of PVDF or PVDF/GO membranes

Fifteen grams of PVDF in the form of powder (molar mass 534,000 g/mol) or granules (molar mass 275,000 g/mol) were dissolved in 80 g of DMAC (molar mass 87.12 g/mol) through magnetic stirring for 24 h at ambient temperature. To improve its mechanical properties and enhance its plasticity and porosity, the polymer matrix was enriched by adding 5 g of the plasticizer (PEG) having a molar mass of 200 g/mol. Then, a 250 μm thick membrane was formed from the casting solution with an Elcometer 3530 mechanical casting knife (the thickness of the membranes was smaller after coagulation). The right membrane size was obtained (about 20 cm × 30 cm). The amount of graphene oxide in the membrane equaled about 0.13 mg/cm^3. In this way produced membrane was conditioned in distilled water for about 24 h. In this manner, a polymer matrix with the reference composition without GO was prepared. As a result, porous and symmetrical membranes (Mem1PVDF534k and Mem3PVDF275k) were obtained. When graphene oxide was added (2 mg), first it was ultrasonically dispersed in 10 g of DMAC for 1 h and mixed with the polymer solution (Mem2PVDF534k+GO and Mem4PVDF275k+GO). Based on previous research, the amount of GO was determined [20]. The fabrication method is schematically shown in Fig. 1.

2.3. Laboratory formation of CA or CA/GO membranes

Fifteen grams of cellulose acetate in the form of powder (molar mass 50,000 g/mol) was dissolved in 80 g of 99% acetic acid (molar mass 60 g/mol), and stirred for 2 h at ambient temperature. Also, in this case, 5 g PEG was added. 250 μm thick CA membrane was formed with the Elcometer 3530 casting knife. In this way, a reference CA membrane was obtained. To obtain a CA/GO membrane, 2 mg of GO was added to the dissolved CA and cut with a knife to the same thickness. As a result, Mem5 and Mem6 were obtained.

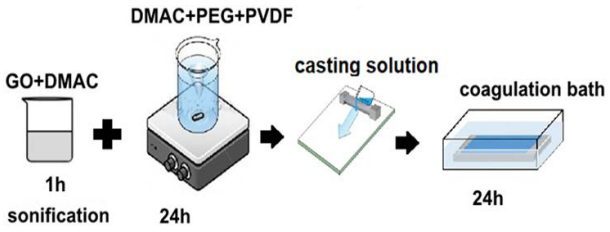

Fig. 1. Preparation of PVDF/GO membrane.

3. Methods of membrane characterization

Preparation of the adequate membrane size allowed determining the properties of three different membrane parts and testing the membrane in the UF process. The prepared membranes were evaluated by determining their thickness, contact angle, the mean pore size, and ultimate tensile strength. Membrane thickness was measured by Micro IP65, the contact angle was assessed using a Surftens-Universal apparatus (Optik, Elektronik&Gerätetechnik mbH, Germany) and pore size distribution (PSD) (3G Porometer Quantachrome). Mechanical properties, that is, Young's modulus [MPa] and tensile strength at break [MPa] were determined with an Instron 3345 tester.

The measurement results are gathered in Table 1.

Fig. 2 shows the changes in the contact angle. As can be noticed, adding GO decreased the contact angle from close to 75° to as low as approximately 43° for PVDF/GO, and from close to 60° to as low as approximately 36° for CA/GO. It was caused by an increase in hydrophilicity of the membrane surface [33].

Membranes were also characterized by determining their porosity. Quantachrome's 3G Porometers employ the method of capillary flow porometry, also known as the

Table 1
Characteristics of the prepared membranes

Membrane	Composition	Thickness (μm)	Contact angle (°)	Young's modulus (MPa)	Tensile strength at break (MPa)	Mean pore size (μm)
Mem1	PVDF534K	105 ± 2	69–75	117 ± 12	0.024 ± 0.005	0.57
Mem2	PVDF534K+GO	115 ± 3	43–48	157 ± 9	0.084 ± 0.002	2.05
Mem3	PVDF275K	105 ± 5	67–70	53 ± 2	0.119 ± 0.007	0.41
Mem4	PVDF275K+GO	112 ± 7	58–61	101 ± 9	0.179 ± 0.005	2.34
Mem5	CA50K	150 ± 10	54–60	53 ± 9	0.015 ± 0.002	1.48
Mem6	CA50K+GO	105 ± 7	36–43	119 ± 9	0.011 ± 0.002	2.43

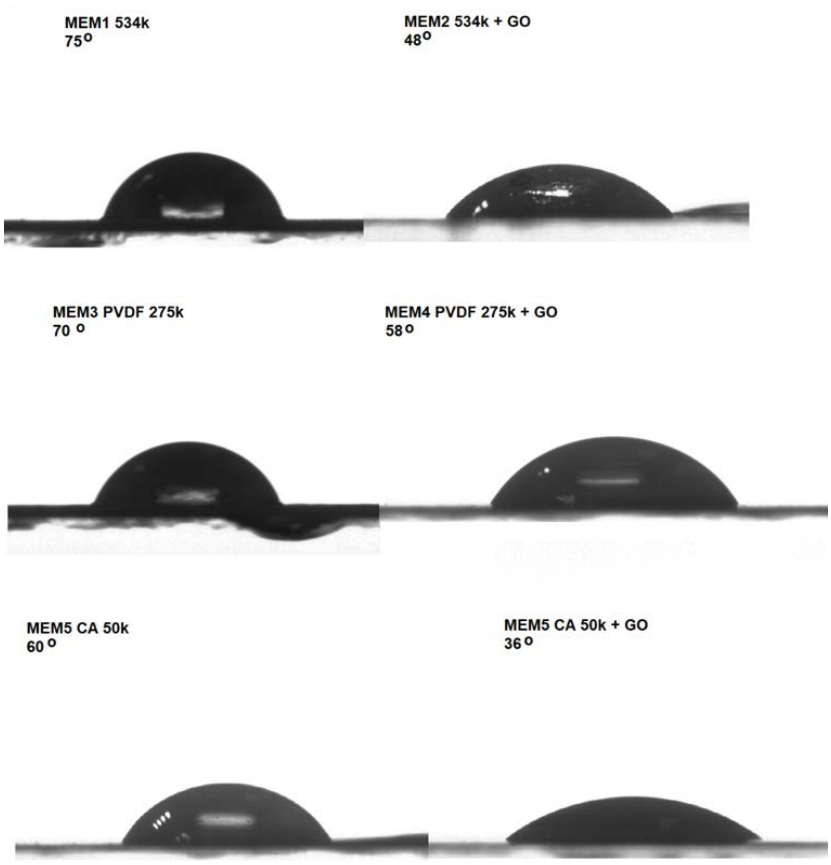

Fig. 2. Decrease in contact angle for GO containing membranes.

liquid expulsion technique, uses the simple principle of gas pressure to force a wetting liquid out of through-pores in a sample. The pressure at which pores empty is inversely proportional to the pore size, larger pores require a lower pressure than do smaller pores. The resulting volumetric flow of gas through emptied pores is also measured. Pore size is calculated using the Washburn equation [Eq. (1)]. The largest pore to be emptied (at the lowest pressure at which flow is sensed) defines the so–called "bubble point." After all, pores have been emptied (up to the highest pressure achievable) during the "wet" run, a second "dry" run is performed on the same sample. From the complete data set, various flow-related pore size parameters, pore size distributions, and gas permeability can be calculated [34].

$$d = \frac{4 \cdot \sigma \cdot \cos\theta}{\Delta P} \cdot 10^{-6} \tag{1}$$

where d is the diameter of the largest pores in the membrane (μm), σ is the surface tension (N/m), θ is the contact angle (°).

An example of pore size distribution (graph of measurements carried out on the porometer) for MEM3 is shown in Fig. 3, and mean pore size in Table 1.

4. UF experiments

The permeability of the membranes was determined in the ultrafiltration process using an OSMONICS KOCH apparatus under transmembrane pressures ranging from 0.1 to 0.6 MPa at 25°C. In the process, a membrane with an area A of 0.002826 m^2 was tested.

The permeability and resistance were made for water and BSA solution.

The volumetric permeation flux was calculated with Eq. (2):

$$J_v = \frac{V}{A \cdot t} \tag{2}$$

where J_v is the volumetric permeation flux (m^3/(m^2 h)), V is the permeate volume (m^3), A is the membrane area (m^2), and t is the time (h).

With knowledge of the permeation flux, the membrane resistance could be determined from Eq. (3):

$$R_m = \frac{\Delta P}{J_v \cdot \eta} \tag{3}$$

where R_m is the hydraulic resistance of the membrane (1/m), ΔP is the transmembrane pressure (Pa), η is the viscosity of water at 25°C (Pa s).

The total resistance R_T in a membrane system is mainly the sum of the membrane R_m and the fouling R_F resistances [Eq. (4)].

$$R_T = R_m + R_F \tag{4}$$

Knowing the total and the membrane resistance it is possible to calculate the fouling resistance.

BSA is often the subject of research because it is one of the proteins that has received a lot of attention regarding its role in pharmaceutical and biotechnological research, and has a defined molar mass. Given the physical and chemical properties of BSA, especially its high molecular weight, it is appropriate to use ultrafiltration to separate this protein [35]. The study involved ultrafiltration tests performed with a dilute solution of BSA (with a molecular

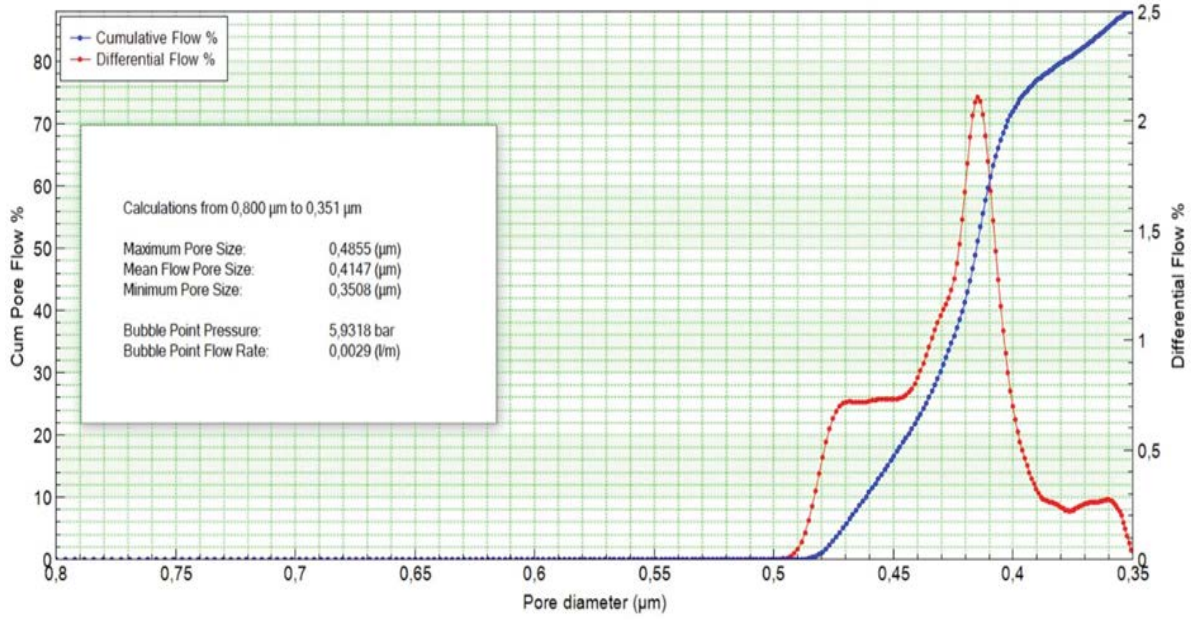

Fig. 3. An example graph for determining the size of pores for MEM3.

weight of 66,430 Da) having a concentration of C_0 = 0.75 g/dm^3 under transmembrane pressures ranging from 1.0 × 10^5 to 6.0 × 10^5 Pa at 25°C. BSA was dissolved in 0.9% NaCl. The BSA content in the permeate and the retentate samples was determined with a spectrophotometric method (Thermo Fisher Scientific spectrophotometer, USA, λ = 279 nm).

In the case of BSA, the rejection coefficient R was calculated from Eq. (5).

$$R = 1 - \frac{C_P}{C_F} \tag{5}$$

where C_F is the feed concentration (mg/dm^3), C_P is the permeate concentration (mg/dm^3).

5. Results and discussion

5.1. Fouling resistances

The most serious problem associated with the membrane filtration process is the pollution of membranes with particles of matter found in aqueous solutions, that is, the phenomenon of fouling. As a result of introducing nanoparticles into the structure of polymer membranes, their separation, and transport properties as well as the phenomenon of fouling change. Blocking the surface and pores of the membrane leads to an increase in the hydraulic resistance of filtration, and to a decrease in the volumetric permeate flux. It was found in Zhao et al. [36] that the addition of GO nanoparticles had a positive effect on the filtered anti-fouling medium properties of the membranes produced. The largest amount of organic contaminants tested, in the form of proteins (BSA) present in the feed, deposited on the unmodified membrane (165.11 mg BSA/m^2), while membranes with the addition of GO had a significantly lower degree of contamination (35.46 mg BSA/m^2). A decrease in permeate flux from the beginning of the UF process was observed for all tested membranes. After 30 min, the flux started to get stabilized. Resistances can be calculated from the water flux through a clean membrane and from BSA permeation flux data [Eq. (2)]. As a result, it is possible to calculate the fouling resistance R_F. The calculation results for MEM4 and MEM6 are presented in Table 2. As the table analysis shows, the main resistance in the ultrafiltration process is associated with the membrane, while the fouling resistance is much lower, especially for PVDF membranes.

5.2. Transport properties PVDF membranes for water and BSA

The usefulness of membranes is demonstrated by high efficiency confirmed by high permeate flux. Therefore, tests are performed for water and the reference compound selected to compare with the results of other researchers. Figs. 4 and 5 show the volumetric permeation fluxes calculated for the PVDF membranes with and without graphene oxide for water and BSA solution. The flux through the membrane with graphene oxide was higher (for both water and BSA) than that of the membrane produced without GO. For the highest pressure water permeation for Mem4 was over 0.18 m^3/(m^2 h), and for Mem2 about 0.16 m^3/(m^2 h). In the case, BSA permeation fluxes were lower for the same

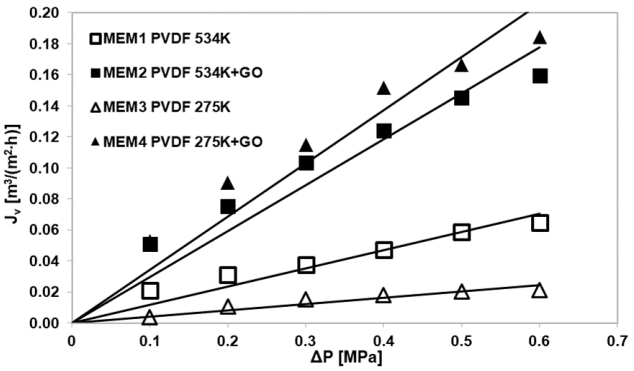

Fig. 4. Volumetric water fluxes for the PVDF membranes are produced with and without the addition of GO vs. transmembrane pressure.

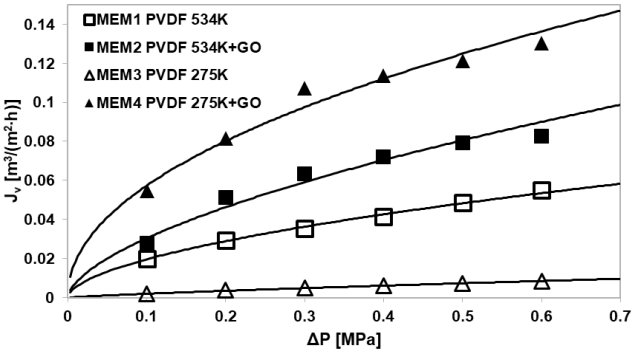

Fig. 5. Volumetric permeate fluxes for the PVDF membranes produced with and without the addition of GO vs. transmembrane pressure for BSA separation.

membranes and were 0.14 m^3/(m^2 h), and 0.10 m^3/(m^2 h), respectively.

5.3. Transport properties CA membranes for water and BSA

Similarly, Fig. 6 presents results obtained for the acetate cellulose membrane with and without graphene oxide. Also, in this case, higher volumetric water fluxes were obtained for the membrane with GO located in the matrix for both water and BSA, 0.11 and 0.08 m^3/(m^2 h), respectively. However, it should be noted that for CA membranes flux values were lower.

5.4. Separation results for manufactured membranes

The retention of the filtered substance is another important factor. The rejection coefficient in membrane processes reaching a level above 50% is already satisfactory. The result reached 90% or higher is definitely outstanding. Fig. 7 illustrates the rejection coefficient R determined for the analyzed BSA solution [Eq. (5)] for 0.1 and 0.6 MPa. The high R-values for PVDV/GO membranes were obtained in this work. The coefficient reached a value of R = 0.90 for the PVDF/GO membrane. The increase in retention was clearly visible compared to membranes without GO.

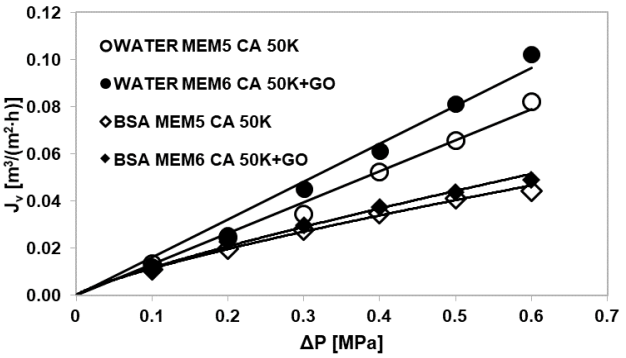

Fig. 6. Comparison of volumetric water or BSA fluxes for the CA membranes with or without GO.

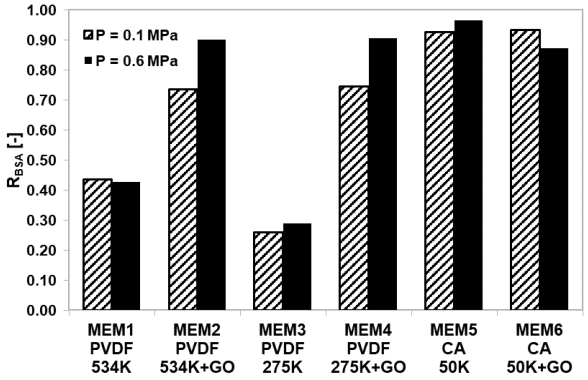

Fig. 7. Comparison of BSA rejection for all membranes at maximum and minimum transmembrane pressure.

Satisfactory retention was also obtained for the CA membrane, but the GO addition did not play a significant role.

6. Summary

The article proposes the preparation of the membranes from two polymers (PVDF and CA) by the phase inversion method with or without GO.

The lab-scale production process resulted in elastic and mechanically durable membranes in both cases. The PVDF or cellulose acetate membranes functionalized graphene oxide have an appropriate pore size distribution for the UF process under transmembrane pressures ranging from 0.1 to 0.6 MPa.

Permeabilities of the produced membranes were compared by determining their water volumetric permeation flux and resistance. It was discovered that the addition of graphene oxide significantly enhanced membrane permeability. The best results were obtained for the MEM4 membrane made of PVDF (molar mass 275,000 g/mol). The PVDF membrane containing graphene oxide provided higher fluxes for water (Mem4: J_v = 0.18 m^3/(m^2 h)) than the membrane without graphene oxide (Mem3: J_v = 0.02 m^3/(m^2 h)).

The same was true for cellulose acetate membranes. J_v = 0.10 m^3/(m^2 h) was obtained for the CA/GO membrane and J_v = 0.08 m^3/(m^2 h) for the CA membrane.

Table 2
Calculated results of transport resistances for produced membranes

ΔP (MPa)	R_T [10^{13} (1/m)]	R_M [10^{13} (1/m)]	R_F [10^{13} (1/m)]
	MEM4 PVDF 275K+GO		
0.2	0.950	0.896	0.054
0.3	1.082	1.055	0.027
0.4	1.365	1.067	0.298
0.5	1.599	1.216	0.383
0.6	1.784	1.315	0.469
	MEM6 CA 50K+GO		
0.2	3.411	3.161	0.250
0.3	3.889	2.687	1.202
0.4	4.122	2.631	1.491
0.5	4.441	2.484	1.957
0.6	4.755	2.367	2.388

It was found that the presence of graphene oxide in the membrane increased hydrophilicity of its surface, which was confirmed by measuring the contact angle and volumetric fluxes increase. The study shows that the addition of graphene oxide causes a substantial (up to a 9-fold for PVDF/GO) increase in the membrane permeability compared with the membranes without GO. For CA/GO membranes, the result was not so spectacular. But it should be stated that the production of CA/GO membranes is easier, does not require the use of organic toxic solvents, and is also more economical.

In the summary should be noted that acceptable high permeability, good BSA rejection of over 90% for PVDF/GO and CA/GO membranes was also obtained. Finally, it can be stated that the results obtained in the presented work were satisfactory especially in the case of PVDF membranes.

In addition, it has been shown that small addition of GO (compared to other papers) significantly increases the volumetric permeate fluxes. At work [37], membranes made of PVDF with the addition of graphene oxide were produced in a similar method to described in this paper. Nevertheless, the mixing of the polymer matrix took place at an elevated temperature (70°C) and not at ambient temperature as was in our experiments. What's more, the content of graphene oxide in the polymer matrix was at the level of 0.1%–0.3%, while GO content in our membranes was only 0.002%, which is more economically justified. It can be seen that the GO addition in the amount of 2 mg/100 g polymer matrix resulted in very similar values of permeate fluxes comparing to the results obtained for the membrane manufactured by Wang et al. [37] with 100 mg GO/100 g.

For example, in the cited work J_v = 0.27m^3/m^2 h (for 0.1 wt.% GO, TMP = 0.1 MPa) and in the presented research J_v = 0.053 m^3/m^2 h (for 0.002 wt.% GO which was a 50-fold smaller GO addition) were obtained. Furthermore, work [37] showed a slight decrease in the contact angle after enrichment of the GO membrane from 79.2° to 63.8° with the addition of 0.3 wt.% GO. For our membrane MEM4 with a 50 times lower GO content, a decrease from 70° to 61° was

obtained. The presented results show that a larger GO addition does not have to increase the permeation and hydrophilicity of the membrane which is compared to articles [38–40].

Symbols

A	—	Membrane area, m^2
C_0	—	Initial concentration, mg/dm^3
C_P	—	Permeate concentration, mg/dm^3
C_F	—	Feed concentration, mg/dm^3
d	—	Diameter of the largest pores in the membrane, μm
J_v	—	Volumetric permeation flux, $m^3/(m^2\ h)$
R_F	—	Fouling resistance, 1/m
R_m	—	Hydraulic resistance of the membrane, 1/m
R_T	—	Total resistance, 1/m
t	—	Time, h
V	—	Permeate volume, m^3
ΔP	—	Transmembrane pressure, Pa
θ	—	Contact angle, °
η	—	Viscosity of water at 25°C, Pa s
σ	—	Surface tension, N/m

References

[1] N.C. Muller, B. Burgen, V. Kueter, P. Luis, T. Melin, W. Pronk, R. Reseiwitz, D. Rickerby, G.M. Rios, W. Wennekes, B. Nowack, Nanofiltration and nanostructured membranes - should they be considered nanotechnology or not?, J. Hazard. Mater., 211–212 (2012) 275–280.

[2] M. Sadeghi, M.A. Semsarzadeh, H. Moadel, Enhancement of the gas separation properties of polybenzimidazole (PBI) membrane by incorporation of silica nano particles, J. Membr. Sci., 331 (2009) 21–30.

[3] J. Hong, Y. He, Effects of nano sized zinc oxide on the performance of PVDF microfiltration membranes, Desalination, 302 (2012) 71–79.

[4] N. Wei, X. Peng, Z. Xu, Understanding water permeation in graphene oxide membranes, ACS Appl. Mater. Interfaces, 6 (2014) 5877−5883.

[5] M. Blus, E. Tomczak, Hydrodynamics of ultrafiltration polymer membranes with carbon nanotubes, Desal. Water Treat., 64 (2017) 298–301.

[6] A. Anand, B. Unnikrishnan, J.-Y. Mao, H.-J. Lin, C.-Ch. Huang, Graphene-based nanofiltration membranes for improving salt rejection, water flux and antifouling–a review, Desalination, 429 (2018) 119–133.

[7] Y. Han, Y. Jiang, C. Gao, High-Flux graphene oxide nanofiltration membrane intercalated by carbon nanotubes, ACS Appl. Mater. Interfaces, 7 (2015) 8147–8155.

[8] Q. Zou, X. Liu, T. Wang, L. Zhang, Enhancement of the thermal stability and mechanical properties of nanocrystalline cellulose/polyvinylidene fluoride ultrafiltration membranes by addition of graphene oxide, Desal. Water Treat., 138 (2019) 1–11.

[9] M. Hu, Z. Cui, J. Li, L. Zhang, Y. Moa, D.S. Dlamini, H. Wang, B. He, J. Li, H. Matsuyama, Ultra-low graphene oxide loading for water permeability, antifouling and antibacterial improvement of polyethersulfone/sulfonated polysulfone ultrafiltration membranes, J. Colloid. Interface Sci., 552 (2019) 319–331.

[10] Z. Li, R.J. Young, R. Wang, F. Yang, L. Hao, W. Jiao, W. Liu, The role of functional groups on graphene oxide in epoxy nanocomposites, Polymer, 54 (2013) 5821–5829.

[11] K. Krishnamoorthya, M. Veerapandian, K. Yun, S.-J. Kim, The chemical and structural analysis of graphene oxide with different degrees of oxidation, Carbon, 53 (2013) 38–49.

[12] T. Tuong Van Tran, S.R. Kumar, S.J. Lue, Separation mechanisms of binary dye mixtures using a PVDF ultrafiltration membrane: Donnan effect and intermolecular interaction, J. Membr. Sci., 575 (2019) 38–49.

[13] H. Yuan, J. Ren, Preparation of poly(vinylidene fluoride) (PVDF)/acetalyzed poly(vinyl alcohol) ultrafiltration membrane with the enhanced hydrophilicity and the anti-fouling property, Chem. Eng. Res. Des., 121 (2017) 348–359.

[14] X. Meng, Y. Ji, G. Yu, Y. Zhai, Preparation and properties of polyvinylidene fluoride nanocomposited membranes based on poly(N-Isopropylacrylamide) modified graphene oxide nanosheets, Polymers, 473 (2019) 1–17.

[15] Y. Zhang, Y. Wang, X. Cao, J. Xue, Q. Zhang, J. Tian, X. Li, X. Qiu, B. Pan, A.Z. Gu, X. Zheng, Effect of carboxyl and hydroxyl groups on adsorptive polysaccharide fouling: a comparative study based on PVDF and graphene oxide (GO) modified PVDF surfaces, J. Membr. Sci., 595 (2020) 1–11.

[16] M. Kumar, Z. Gholamvand, A. Morrissey, K. Nolan, M. Ulbricht, J. Lawler, Preparation and characterization of low fouling novel hybrid ultrafiltration membranes based on the blends of GO–TiO_2 nanocomposite and polysulfone for humic acid removal, J. Membr. Sci., 506 (2016) 38–49.

[17] Z. Qiu, X. Kong, J. Yuan, Y. Shen, B. Zhu, L. Zhu, Z. Yao, C. Tang, Cross-linked PVC/hyperbranched polyester composite hollow fiber membranes for dye removal, React. Funct. Polym., 122 (2018) 51–59.

[18] G. Kang, Y. Cao, Application and modification of poly(vinylidene fluoride) (PVDF) membranes–a review, J. Membr. Sci., 463 (2014) 145–165.

[19] Z. Rahimi, A.A. Zinatizadeh, S. Zinadini, Membrane bioreactorstroubleshooting through the preparation of a high antifouling PVDF ultrafiltration mixed-matrix membrane blended with O-carboxymethyl chitosan-Fe_3O_4 nanoparticles, Environ. Technol., 40 (2019) 3523–3533.

[20] E. Tomczak, M. Blus, Preparation and permeability of PVDF membranes functionalized with graphene oxide, Desal. Water Treat., 128 (2018) 20–26.

[21] L.-G. Wu, X.-Y. Zhang, T. Wang, C.-H. Du, C.-H. Yang, Enhanced performance of polyvinylidene fluoride ultrafiltration membranes by incorporating TiO_2/graphene oxide, Chem. Eng. Res. Des., 141 (2019) 492–501.

[22] B. Saini, M.K. Sinha, S.K. Dash, Mitigation of HA, BSA and oil/water emulsion fouling of PVDF ultrafiltration membranes by SiO_2-g-PEGMA nanoparticles, J. Water Process. Eng., 30 (2019) 100603, doi: 10.1016/j.jwpe.2018.03.018.

[23] H. Liu, X. Liu, F. Zhao, Y. Liu, L. Liu, L. Wang, C. Geng, P. Huang, Preparation of a hydrophilic and antibacterial dual function ultrafiltration membrane with quaternized graphene oxide as a modifier, J. Colloid Interface Sci., 562 (2020) 182–192.

[24] S. Devi, P. Ray, K. Singh, P.S. Singh, Preparation and characterization of highly micro-porous PVDF membranes for desalination of saline water through vacuum membrane distillation, Desalination, 346 (2014) 9–18.

[25] A. Abdel-Karim, J.M. Luque-Alled, S. Leaper, M. Alberto, X. Fan, A. Vijayaraghavan, T.A. Gad-Allahb, A.S. El-Kalliny, G. Szekely, S.I.A.Ahmed, S.M.Holmes, P. Gorgojo, PVDF membranes containing reduced graphene oxide: effect of degree of reduction on membrane distillation performance, Desalination, 452 (2019) 196–207.

[26] S.M. Ghaseminezhad, M. Barikani, M. Salehirad, Development of graphene oxide-cellulose acetate nanocomposite reverse osmosis membrane for seawater desalination, Composites, Part B, 161 (2019) 320–327.

[27] D.D. Fazullin, R.D. Fazylova, Purification of water from heavy metal ions by a dynamic membrane with a surface layer of cellulose acetate, IOP Conf. Ser.: Earth Environ. Sci., 421 (2020) 1–5, doi:10.1088/1755–1315/421/6/062032.

[28] D.D. Fazullin, G.V. Mavrin, Separation of water-oil emulsions using composite membranes with a cellulose acetate surface layer, Chem. Pet. Eng., 55 (2019) 649–656.

[29] A. Shams, S.A. Mirbagheri, Y. Jahani, The synergistic effect of graphene oxide and POSS in mixed matrix membranes for desalination, Desalination, 472 (2019) 1–10.

[30] A. Shams, S.A. Mirbagheri, Y. Jahani, Effect of graphene oxide on desalination performance of cellulose acetate mixed matrix membrane, Desal. Water Treat., 164 (2019) 62–74.

[31] S. Nurkhamidah, B.C. Devi, B.A. Febriansyah, A. Ramadhani, R.D. Nyamiati, Y. Rahmawati, A. Chafidz, Characteristics of cellulose acetate/polyethylene glycol membrane with the addition of graphene oxide by using surface coating method, IOP Conf. Ser.: Mater. Sci. Eng., 732 (2020) 1–6.
[32] S. Yang, Q. Zou, T. Wang, L. Zhang, Effects of GO and MOF@GO on the permeation and antifouling properties of cellulose acetate ultrafiltration membrane, J. Membr. Sci., 569 (2019) 48–59.
[33] B.M. Ganesh, A.M. Isloor, A.F. Ismail, Enhanced hydrophilicity and salt rejection study of graphene oxide-polysulfone mixed matrix membrane, Desalination, 313 (2013) 199–207.
[34] Available at: https://www.quantachrome.com/technologies/porometry.html
[35] N. Alia, H. Sofiah, A. Asmadi, A. Endut, Preparation and characterization of a polysulfone ultrafiltration membrane for bovine serum albumin separation: effect of polymer concentration, Desal. Water Treat., 32 (2011) 248–255.
[36] C. Zhao, X. Xu, J. Chen, F. Yang, Effect of graphene oxide concentration on the morphologies and antifouling properties of PVDF ultrafiltration membranes, J. Environ. Chem Eng., 1 (2013) 349–354.
[37] Z. Wang, H. Yu, J. Xia, F. Zhang, F. Li, Y. Xia, Y. Li, Novel GO-blended PVDF ultrafiltration membranes, Desalination, 299 (2012) 50–54.
[38] S. Xia, M. Ni, Preparation of poly(vinylidene fluoride) membranes with graphene oxide addition for natural organic matter removal, J. Membr. Sci., 473 (2015) 54–62.
[39] W.C. Chong, E. Mahmoudi, Y.T. Chung, C.H. Koo, A.W. Mohammad, K.F. Kamarudin, Improving performance in algal organic matter filtration using polyvinylidene fluoride–graphene oxide nanohybrid membranes, Algal Res., 27 (2017) 32–42.
[40] J. Zhang, Z. Xu, M. Shan, B. Zhou, Y. Li, B. Li, J. Niu, X. Qian, Synergetic effects of oxidized carbon nanotubes and graphene oxide on fouling control and anti-fouling mechanism of polyvinylidene fluoride ultrafiltration membranes, J. Membr. Sci., 448 (2013) 81–92.